Appl. Phys. A 73, 67–73 (2001) / Digital Object Identifier (DOI) 10.1007/s003390100833

Applied Physics A
Materials
Science & Processing

Synthesis of nanocrystalline material by sputtering and laser ablation at low temperatures

P. Ayyub*, **R. Chandra****, **P. Taneja**, **A.K. Sharma*****, **R. Pinto**

Department of Condensed Matter Physics and Materials Science, Tata Institute of Fundamental Research, Mumbai 400 005, India

Received: 31 October 2000/Accepted: 9 January 2001/Published online: 26 April 2001 – © Springer-Verlag 2001

Abstract. Physical vapor deposition techniques such as sputtering and laser ablation – which are very commonly used in thin film technology – appear to hold much promise for the synthesis of nanocrystalline thin films as well as loosely aggregated nanoparticles. We present a systematic study of the process parameters that facilitate the growth of nanocrystalline metals and oxides. The systems studied include TiO_2, ZnO, γ-Al_2O_3, Cu_2O, Ag and Cu. The mean particle size and crystallographic orientation are influenced mainly by the sputtering power, the substrate temperature and the nature, pressure and flow rate of the sputtering gas. In general, nanocrystalline thin films were formed at or close to 300 K, while loosely adhering nanoparticles were deposited at lower temperatures.

PACS: 73.61.Tm; 81.05.Ys; 81.15.Cd; 81.15.Fg

During the last decade, research involving nanophase materials has shown an unprecedented growth because such materials possess unique properties that are often superior to those of conventional large-grained polycrystalline materials. For example, nanophase materials may exhibit increased hardness, higher electrical resistivity, lower thermal conductivity, greater specific heat, higher thermal expansion coefficients and superior soft magnetic properties [1–5]. Such materials are also of great interest in the basic sciences, since a reduction in the crystallite size may produce substantial changes in structural, magnetic, optical, dielectric, thermal and other physico-chemical properties. We can broadly define a nanophase material as one in which the average crystallographic domain size falls in the range 1–50 nm. They include nanocomposites, loosely aggregated nanoparticles, cluster-assembled materials, sintered materials with an ultrafine grain structure and nanocrystalline thin films. In addition, these materials include precisely engineered semiconductor nanostructures such as quantum dots, wires and wells.

Depending on the size range of interest and the material involved, different types of synthetic techniques have been utilized to prepare nanophase materials. These include wet chemical processes, spray techniques and physical vapor deposition (PVD) methods. Of these, wet chemical techniques such as co-precipitation, complexation and sol-gel are probably the most popular, mainly for operational reasons. However, it is becoming increasingly clear that for certain applications, PVD methods hold distinct advantages over chemical ones. For example, a uniform, nearly monodisperse array of metallic or metal oxide nanoparticles deposited on a suitable substrate may have important applications such as in heterogeneous catalysis, gas sensor technology and microelectronics. When such structures are required, wet synthetic techniques may be unsuitable because they need a final calcination step. This not only leads to a growth in the particle size, but also causes a broadening of the size distribution due to thermal agglomeration. Clearly, in such cases, a process that can be carried out at or below room temperature would be greatly advantageous. In this paper, we investigate the use of high-pressure magnetron sputtering and laser ablation in the synthesis of nanocrystalline thin films under controlled conditions, at low temperatures and (in most cases) without the need for post-annealing. Both techniques are widely used in thin film technology, but their potential in nanotechnology remains virtually untapped.

Our studies on a number of different nanomaterial systems synthesized by these techniques show that by proper choice of the process parameters, it is possible to obtain a wide range of sizes, starting from 3–5 nm, and the size distribution is reasonably narrow. Smooth and adherent nanocrystalline films can be formed on many different types of substrates such as glass, quartz, Si wafers, $LaAlO_3$, $SrTiO_3$ and polished metals. At low enough temperatures, it is also possible to synthesize loosely aggregated nanoparticles that can be compacted in situ to obtain a nano-grained matrix.

Compacted nanomaterials are often produced by inert gas condensation of resistively heat-evaporated samples [6]. However, sputtering and laser ablation have the following

*Corresponding author. (Fax: +91-22/215-2110, E-mail: pushan@tifr.res.in)
***Current address: Department of Physics, Guru Nanak Dev University, Amritsar 143005, India*
****Current address: Department of Materials Science and Engineering, North Carolina State University, Raleigh, NC 27695, USA*

important advantages over thermal evaporation: (1) During heating, some metals may react with the refractory crucibles. Also, if a metal crucible is used, it may oxidize and contaminate the sample. (2) Sputtering and laser ablation can both be used for a large number of metals, semiconductors and insulators, but resistive heating is severely limited to metals and simple alloys and oxides. (3) In a molten metal, the temperature distribution is often non-uniform, therefore exact reproducibility is difficult. The conditions during sputtering and laser ablation can usually be controlled fairly well. (4) In the case of multi-component systems, the stoichiometry of the sputtered [7] as well as the ablated material [8] is known to closely resemble that of the target. However, the exact composition of alloys and compounds is generally not maintained during thermal evaporation. This is the major advantage of these techniques over thermal evaporation. The feasibility of using sputtering for nanoparticle synthesis has been demonstrated in earlier studies [9–11].

1 Experiments

1.1 High-pressure sputtering

A schematic diagram of the basic experimental system for sputtering of nanoparticles is shown in Fig. 1. Options for both dc and RF sputtering were provided so as to accommodate a wide variety of samples. A 200 mm long axial planar magnetron sputtering source (Atom Tech 320-O) suitable for 50 mm diameter targets was used. This source can operate at the maximum input power level of 1 kW (dc) or 600 W (RF), though the average power levels used were much smaller (typically 50–200 W). The sputter source was fed either by a Glassman LV series dc power supply (0–600 V $\pm$ 300 mV, 0–1.7 A $\pm$ 0.85 mA) or by a RF Plasma Products power supply (1 kW at 13.56 MHz $\pm$ 0.05%) coupled with an MN-500 manual matching network.

The custom-designed vacuum chamber (30 cm diameter and 30 cm tall) with 8 ports (whose functions are indicated in Fig. 1) was initially evacuated to $\approx 10^{-6}$ Torr by a Varian turbo-molecular pump. A highly pure inert gas (He, Ne, Ar, Kr or Xe were all used) at a constant, pre-selected pressure – typically between 5 and 200 mTorr – was then allowed into the chamber, and sputtering was carried out in flowing gas. The substrate was securely fixed to the copper cold finger of a liquid nitrogen cryostat and held at a distance of 5–7.5 cm from the sputtering target. Different types of substrates (such as glass, quartz, silicon wafer, copper or stainless steel) were successfully used. Both horizontal as well as vertical (bottom upwards) sputtering geometries can be used to deposit nanocrystalline thin films. However, during the deposition of loosely aggregated nanoparticles at low temperature, it was found preferable to use a horizontal geometry and keep a Petri dish below the substrate to collect the particles that fell off the substrate. When the cryostat was filled with liquid nitrogen (L-N_2), the actual temperature of the substrate was found to be about 120 K. Care was taken to ensure that the substrate temperature increased by only a few degrees (≤ 5 K) during sputtering.

The ambient pressure was typically maintained at values higher than those required in thin film processing to ensure substantial collision between the sputtered atoms and the inert gas atoms. This leads to cluster formation and reduces the mean energy with which these clusters approach the substrate. On the other hand, the substrate was held at temperatures much lower than in thin film formation (typically 100–300 K). This tends to inhibit grain growth in the plane of the film and allows the production of nanoparticles as well as nanocrystalline thin films. Contamination due to the possible diffusion of atoms from the substrate to the sample is also minimized at the low operational temperatures.

1.2 Laser ablation

In pulsed laser ablated deposition (PLD), a short-wavelength high-power laser is directed at a solid target, producing an energetic beam of charged as well as neutral clusters of atoms. We used a 248 nm KrF excimer laser (Lambda Physik), operated with a pulse repetition rate of 10 Hz and a pulse width of

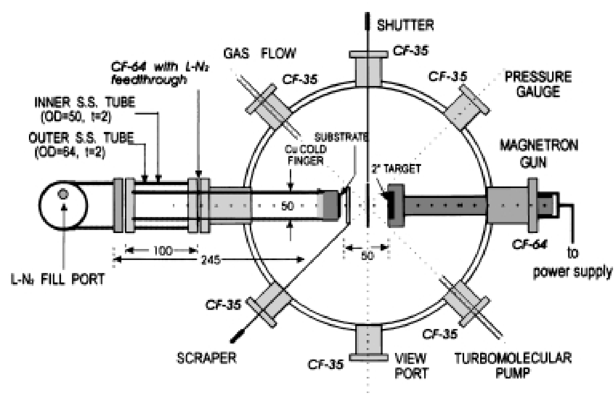

Fig. 1. Schematic diagram (not to scale) of a low-temperature magnetron sputtering system used for the synthesis of nanoparticles and nanocrystalline thin films

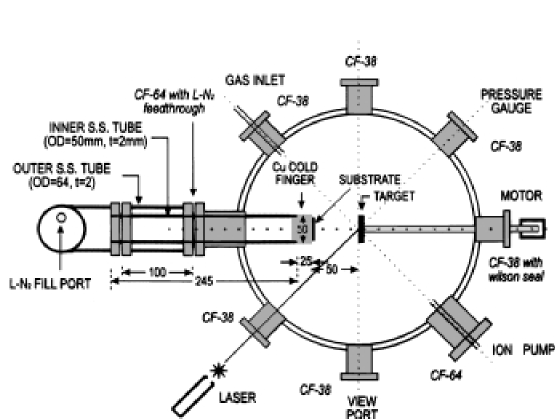

Fig. 2. Schematic diagram (not to scale) of a low-temperature laser ablation system used for nanoparticle synthesis

25 ns. During the PLD process, local heating of the target was minimized by scanning the laser beam across the target with the help of a stepper-motor–controlled oscillatory scanner. The laser ablation chamber is shown in Fig. 2. The ablated material was collected on a 50 mm-diameter stainless-steel disc. As before, the temperature of the sample holder was kept low (with the help of a liquid nitrogen cryostat) in order to prevent the growth of continuous films. For the synthesis of oxide nanoparticles, ablation was done in a relatively high pressure of pure oxygen (0.2–0.8 Torr), after initially evacuating the chamber. The nominal laser energy was in the range 0.4–0.8 J (corresponding to a laser fluence of 5.0 and 10.0 J cm^{-2}).

1.3 Particle size analysis

The morphology and particle size distribution in the nanocrystalline samples were studied by standard techniques such as transmission electron microscopy (TEM) and atomic force microscopy (AFM). The mean particle size was determined in terms of the coherently diffracting crystallographic domain size (d_{XRD}) from X-ray diffraction line broadening (Scherrer technique), after correcting for instrumental broadening.

2 Results and discussions

2.1 TiO_2

Nanocrystalline TiO_2 was prepared using both laser ablation and dc-sputtering at low temperatures. For laser ablation, the targets used were 25 mm-diameter pellets of TiO_2 in two of its common crystallographic modifications: anatase (tetragonal, $I4_1/amd$) and rutile (tetragonal, $P4_2/mnm$). Anatase converts irreversibly to rutile when heated above ≈ 1000 °C. The anatase pellets were prepared by sintering 99.9% pure anatase (Merck) at 900 °C, while the rutile pellets were prepared by sintering the same material at 1200 °C. Deposition of TiO_2 occurred only when the pressure of the ambient oxygen was below 0.8 Torr, and optimal deposition took place when the oxygen pressure was in the range 0.20–0.65 Torr.

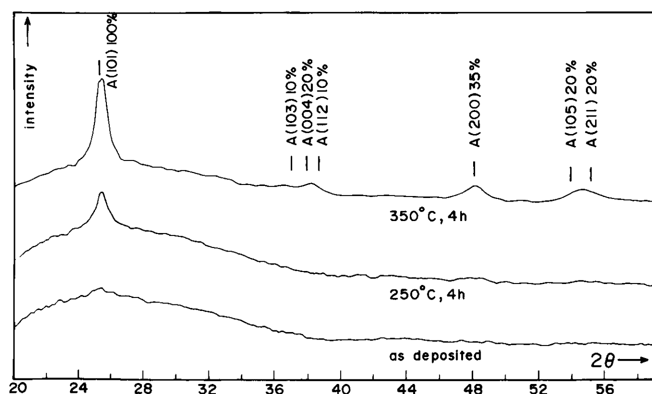

Fig. 3. X-ray diffractograms (XRD) of a nanocrystalline TiO_2 sample produced by laser ablation from a rutile target at a nominal energy of 0.65 J, under an oxygen pressure of 0.2 Torr. The temperature of the sample holder was 120 K. The XRD from the as-deposited amorphous sample is shown at the *bottom*. This can be converted to nanocrystalline anatase ($d_{XRD} = 10$ nm) on heating to 350 °C for 4 h. Each anatase peak is marked with “A”, followed by the (*hkl*) index and the expected relative intensity (%)

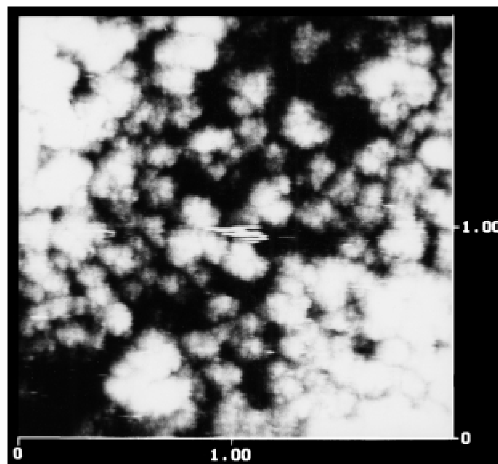

Fig. 4. Atomic force micrograph (area covered = 2 μm × 2 μm) of as-sputtered, amorphous nanoparticles of TiO_2, deposited on a liquid nitrogen-cooled substrate

The most interesting result of this study was the distinct and systematic difference in the ablation products from rutile and anatase. With rutile as the ablation target, the product deposited on the L-N_2 cooled substrate was always amorphous, nanoparticulate TiO_2. On collecting this sample and heating it ex situ at 350 °C for 4 h, it converts to nanocrystalline anatase with $d_{XRD} \approx 10$ nm (see Fig. 3), though a small amount of residual amorphous phase cannot be ruled out. Such a conversion from rutile to anatase with a decrease in the particle size is in accordance with earlier observations, such as on microemulsion-derived TiO_2 nanoparticles [12], in which it was shown that smaller precursor particles tend to produce the anatase phase in preference to the rutile phase. However, when anatase itself was used as a target (other conditions remaining the same), the collected sample consisted of a mixture of relatively larger particles (50–100 nm) of anatase, rutile and amorphous TiO_2. At present, we have no obvious explanation for this type of behavior. It is possible that the difference in their ablation characteristics arises partly from the rutile pellet being more fully sintered (since it was heated at a higher temperature) than the anatase pellet.

Nanocrystalline TiO_2 was also produced by dc-sputtering from a target of 99.9% pure metallic Ti. The sputtering gas was a flowing mixture of Argon (95%) and oxygen (5%) at a pressure of 20 mTorr. The stainless-steel sample collection plate was maintained nominally at L-N_2 temperature, at a distance of 5 cm from the target. The sputtering power was 66 W (284 V, 234 mA). The as-collected ultrafine powder was amorphous (as in the case of laser ablation from rutile) and could be heated in air to obtain ultrafine particles of anatase. The nanocrystalline nature of the as-collected TiO_2 material can be clearly seen in the AFM picture in Fig. 4.

2.2 ZnO

The target used for the synthesis of nanocrystalline ZnO by laser ablation was a pellet of ZnO (99.99%) sintered at 1000 °C for 10 h. Laser ablation was carried out in an oxygen atmosphere, and the nanocrystalline material produced

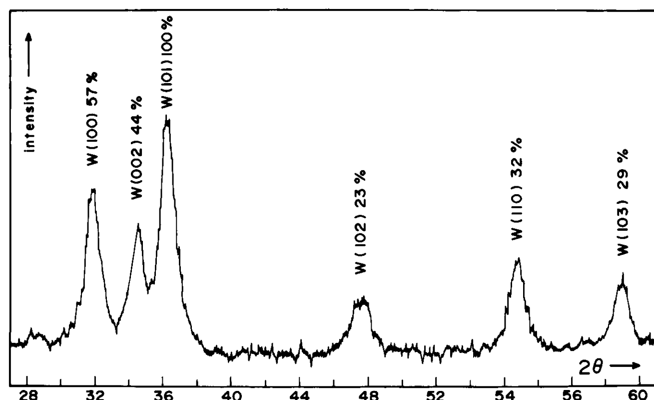

Fig. 5. X-ray diffraction spectra of as-deposited nanocrystalline (d_{XRD} = 8 nm) ZnO produced by laser ablation from a ZnO target at a nominal energy of 0.45 J, under an oxygen pressure of 0.6 Torr. The temperature of the sample holder was 120 K. Each ZnO peak (wurtzite phase) is marked with "W", followed by the (*hkl*) index and the expected relative intensity (%)

was collected on a cooled substrate. The resulting crystallographic phase and particle size were analyzed as a function of: (i) the incident laser energy, which varied in the range 0.4–0.8 J; and (ii) the ambient oxygen pressure, which varied in the range 0.1–0.6 Torr. The commonly occurring wurtzite phase of ZnO started forming only when the oxygen pressure was above 0.4 Torr. Impurity phases were also found when the laser energy was too high. Single-phase nanocrystalline (d_{XRD} = 8 nm) ZnO was formed at a (nominal) laser energy of 0.45 J and an oxygen pressure of 0.6 Torr. The XRD spectrum of this sample is shown in Fig. 5.

2.3 Cu_2O

Cu_2O is a *p*-type semiconductor and is considered a promising candidate for photovoltaic applications [13]. In many earlier studies, there are reports of the difficulty in producing phase-pure nanocrystalline Cu_2O, uncontaminated by CuO. Initially, we tried to synthesize Cu_2O nanoparticles by laser ablation from a CuO pellet at low temperature. This was based on an earlier observation that CuO converts to Cu_2O with decreasing particle size [14]. For an oxygen pressure of 0.5 Torr and a laser energy of 0.5 J, the majority phase in the ablated product was indeed Cu_2O. However, within the parameter space we explored, we did not succeed in producing perfectly single-phase nanocrystalline Cu_2O by laser ablation.

Dc-sputtering from a metallic copper target (99.99% pure) turns out be a more useful technique in this case. By proper selection of the pressure of the sputter gas it was possible to produce pure Cu as well as pure Cu_2O, both in the nanocrystalline form. In general, monophasic, nanocrystalline Cu_2O could be produced by dc-sputtering (at a power of 50 W) in 100–200 mTorr of pure Ar. The crystallite size (d_{XRD}) could be controlled in the range 5–50 nm by proper choice of gas pressure and substrate temperature. As expected, the substrate temperature (T_S) plays a very significant role. At $T_S = 300$ K, one obtains nanocrystalline thin films with shiny surfaces and good adherence to various substrates such as Si, glass and quartz. At $T_S = 120$ K, however, the deposited material is particulate and loosely aggregated. We emphasize that the oxidation of Cu to form Cu_2O occurs merely via reaction with the residual oxygen in the ambient atmosphere and in the sputtering gas (Ar, with a nominal purity of 99.999%). Formation of pure Cu_2O occurs at relatively high pressure($\geq$ 100 mTorr). The most likely mechanism for Cu_2O formation appears to be surface oxidation of the Cu nanoparticles since the cold substrate acts as an efficient trap for both oxygen and water vapour even at quite low ($\sim$ 10 ppm) impurity levels. Metallic copper is formed at lower Ar pressure (below 10 mTorr). At intermediate gas pressures, a mixture of metallic Cu and Cu_2O is obtained. However, when sputtering was done in an Ar-O_2 gas mixture (95%Ar + 5%O_2), the deposited sample had a substantial fraction of CuO.

X-ray diffraction patterns of as-deposited nanocrystalline Cu_2O thin films are shown in Fig. 6. At the same pressure of Ar gas (200 mTorr) it is possible to obtain either completely (111)-aligned (top) or randomly oriented (center) Cu_2O nanoparticles, by an appropriate choice of the gas flow rate.

Using Cu_2O as a model system, the effect of the various process parameters on the average particle size and morphology of the deposited nanomaterial system was studied in detail. For example, the effect of the sputtering gas was observed by depositing Cu_2O at 300 K in 100 mTorr of He, Ne, Ar, Kr and Xe, separately, keeping the dc power and geometric parameters unaltered. Compact nanocrystalline thin films with smooth surfaces and good adhesion (to the Si substrate) were formed in each case. However, the grain size depended on the nature of the ambient gas. AFM results indicate (Fig. 7) a slight but systematic decrease in the average grain (aggregate) size with an increase in the atomic mass of the inert gas. However, the variation in the X-ray domain size (d_{XRD}) shows the opposite trend. The X-ray domain size increases from 8 nm (in He) through 10 nm (in Ar) to 14 nm (in Xe). The XRD and AFM data can be reconciled by the fact that smaller primary particles have a larger surface free energy and would, therefore, tend to agglomerate faster and grow into larger grains

The fact that high-quality nanocrystalline thin films of Cu_2O could be grown on various standard substrates such as

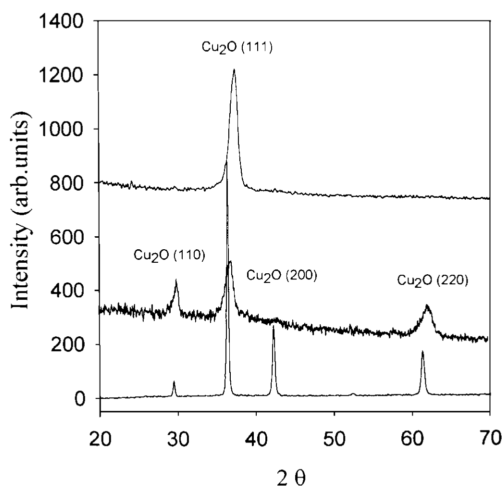

Fig. 6. X-ray diffraction spectra of nanocrystalline Cu_2O sputter-deposited at room temperature in 200 mTorr Ar (*top* and *center*). The spectrum at the top is from a sample deposited at a higher gas flow rate. The comparison spectrum at the bottom is from bulk, polycrystalline Cu_2O

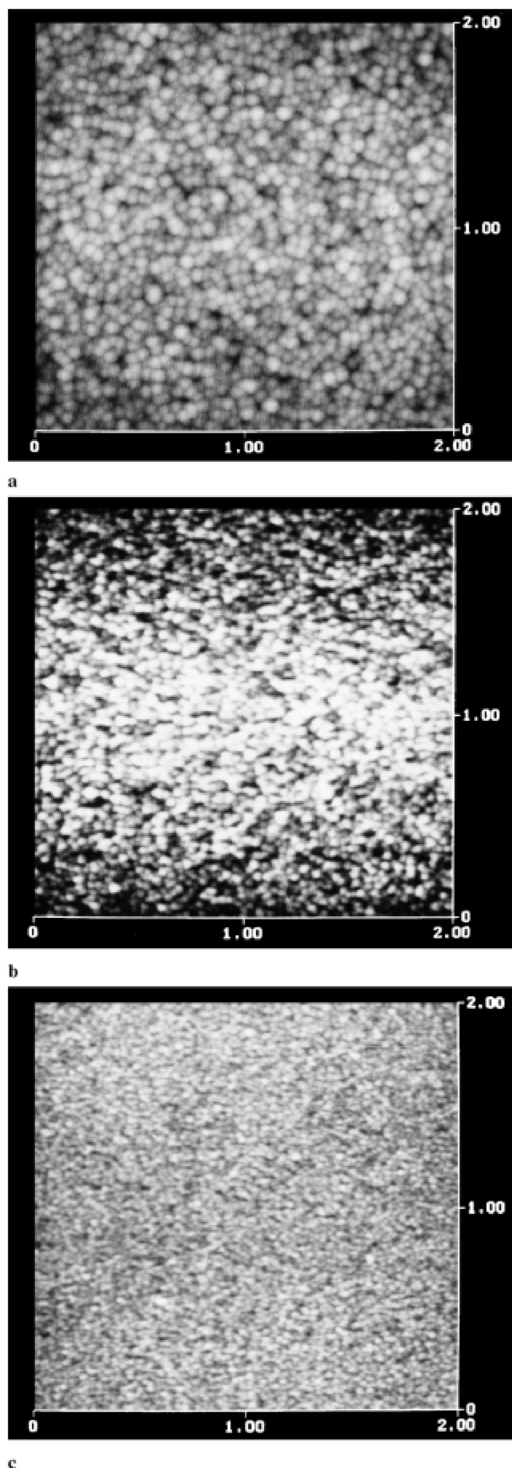

Fig. 7a–c. Atomic force micrographs from $2\,\mu m \times 2\,\mu m$ surface of nanocrystalline Cu_2O thin films sputter-deposited in **a** He, **b** Ar and **c** Xe gases, respectively, at room temperature under otherwise identical conditions (100 mTorr, 50 W)

quartz, glass, $LaAlO_3$ and MgO, in addition to Si wafers is of technological interest. The grain morphology is relatively independent of the nature of the substrate and is controlled more by the sputtering parameters. A detailed study of the optical properties of quasi-transparent nano-Cu_2O is reported elsewhere [15].

2.4 γ- Al_2O_3

Nanocrystalline γ-alumina (γ-Al_2O_3) is a technologically important material that is used, for example, as a catalyst support and as an adsorbent. Earlier studies have established that the γ-phase of alumina is preferentially nucleated at the smallest particle sizes [16]. We synthesized γ-Al_2O_3 by dc-sputtering from a 99.999% pure Al target in an atmosphere of argon. The base pressure was 2×10^{-6} Torr and sputtering was done in 15 mTorr of Ar at 330 V and 180 mA. The substrate was cooled by liquid nitrogen. The as-deposited nanoparticulate sample was amorphous to XRD. However, it could be converted to single-phase greyish-white nanocrystalline γ-Al_2O_3 on post-annealing at 900 °C for 1 h. The XRD pattern of this sample is shown in Fig. 8. The X-ray domain size of the annealed γ-Al_2O_3 phase was found to be $d_{XRD} = 10$ nm.

2.5 Metallic Cu *and* Ag *nanoparticles*

Metallic copper nanoparticles can be formed by dc-sputtering at low inert gas pressure (below 5–10 mTorr), at temperatures in the range 100–300 K. At such pressures, the motion of the sputtered Cu atoms is expected to be mainly ballistic. At higher pressure, the motion becomes increasingly diffusive, and the residual oxygen in the ambient tends to oxidize the Cu atoms to Cu_2O, as described above.

Nanocrystalline silver can be directly formed over a wide range of inert gas pressures (5–600 mTorr) and substrate temperatures (100–300 K). The primary particle size (d_{XRD}) can be controlled in the approximate range 5–50 nm by appropriate choice of sputtering parameters. At room temperature, one obtains nanocrystalline thin films of both Ag and Cu with a smooth, metallic finish. At L-N_2 temperature, the material deposited is powdery with relatively poor adhesion, but the value of d_{XRD} obtained (other conditions being identical) is consistently lower than at 300 K. In some cases, it is possible to control the crystallographic orientation of the deposited particles. Our studies indicate that the orientation along a preferred growth direction is encouraged by higher sputtering gas pressure and lower substrate temperature. Figure 9 shows XRD spectra of (111)-oriented (200 mTorr Ar) and randomly oriented (150 mTorr Ar) Ag nanoparticles, both deposited at ≈ 120 K.

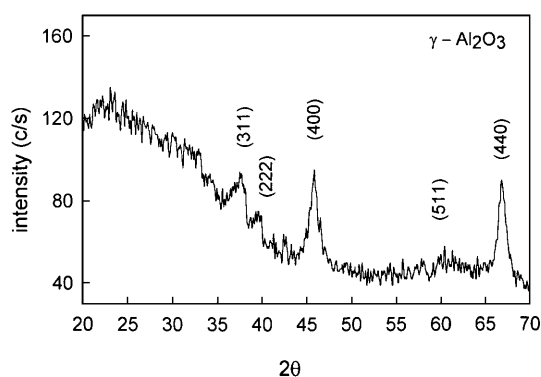

Fig. 8. X-ray diffraction spectra for sputter-deposited and post-annealed (900 °C, 1 h) γ-Al_2O_3 in nanocrystalline form. The indexes are based on the cubic γ-Al_2O_3 phase. The large amorphous background centered $2\theta = 24°$ comes from the glass substrate

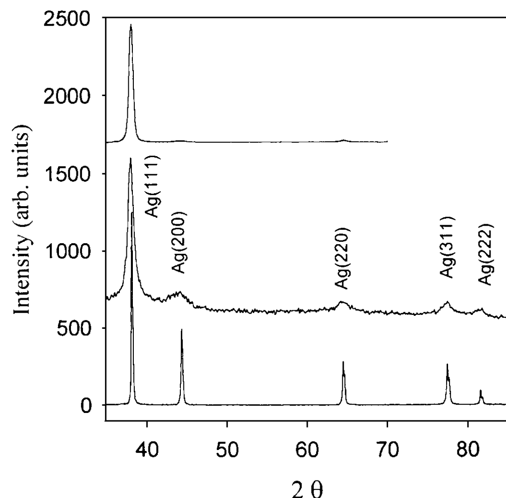

Fig. 9. X-ray diffraction spectra of nanocrystalline silver deposited at liquid nitrogen temperature, using a sputtering power of about 50 W. The *top spectrum* shows a (111) oriented nanocrystalline thin film deposited at 200 mTorr Ar, while a spectrum for a randomly oriented nanocrystalline thin film deposited at 150 mTorr is shown at the center. XRD data for bulk silver is shown for comparison at the *bottom*

A detailed study of the effect of sputtering parameters such as substrate temperature, gas pressure, sputtering voltage and current indicate that the observed particle size is controlled by several competing processes. This is indicated by the observed non-monotonic dependence of the sputter current on the ambient gas pressure. One needs to consider the kinetic energy with which the atoms and clusters arrive at the substrate (which depends on both the sputter voltage and the gas pressure) and the substrate temperature, as well as the rate of heat dissipation. The rate at which the particles arrive at the substrate (which is related to the current) is the other important factor. As an illustration, the dependence of the average particle size in nanocrystalline Ag on the pressure of the ambient gas (at constant voltage) for two different substrate temperatures is shown in Fig. 10.

The ultimate aim of this type of study should be to describe the nanostructure evolution in terms of a structure-zone scheme such as the one suggested by Thornton [17]. Such a scheme would have to be extended to higher pressures. This is a non-trivial extension since the sputtering current shows a non-monotonic dependence on the ambient pressure at higher pressures. One must also attempt to consider the effect of sputtering voltage (or power) on the nanostructure within the framework of such a scheme. In terms of Thornton's model, the sputter deposition of silver (under moderate pressures) at ≈ 100 K would fall in Zone I, in which we would expect equi-axed grains with $d < 20$ nm. However, samples deposited at 300 K could fall in either Zone 2 or Zone T (transition). In Zone 2, at low pressures, one may expect granular epitaxy with columnar grains. Such is the case with the low pressure (5 mTorr) sample that shows a comparatively large "particle size" (d_{XRD}) in Fig. 10. This can be ascribed to columnar growth along the $\langle 111 \rangle$ direction.

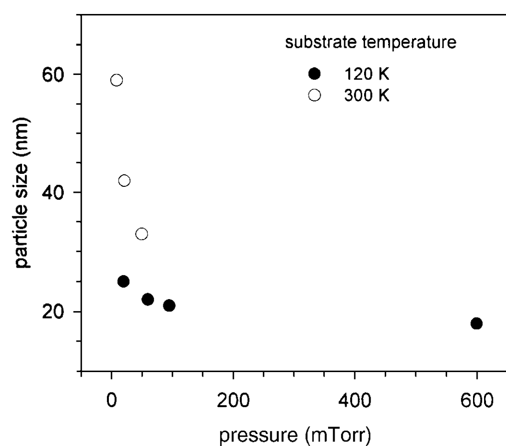

Fig. 10. Dependence of X-ray domain size (d_{XRD}) of nanocrystalline silver on argon gas pressure. The sputtering voltage was constant at 230 V and the substrate (Si) was maintained either at 300 K or at 120 K

3 Conclusions

It is possible to produce nanoparticles and nanocrystalline thin films of a wide range of simple oxides and some pure metals by physical vapor deposition techniques such as sputtering and laser ablation. Comparatively high gas pressures (10–200 mTorr) and low substrate temperatures (100–300 K) are used to discourage the formation of continuous thin films. Of the two techniques, dc/RF sputtering generally appears to provide better control over the chemical phase, mean size and crystallographic orientation of the nanocrystalline product. Within the parameter space investigated in this study, the following trends are fairly obvious:

(a) Lower substrate temperatures promote smaller particle sizes. In most cases, coherent, nanocrystalline thin films with good adhesion properties are formed close to room temperature, while loosely aggregated nanoparticles with poorer adhesion are more likely to occur at lower temperatures. Not only does a lower substrate temperature prevent inter-particle aggregation, it also provides a thermal gradient that encourages the condensation of the sputtered species.
(b) At constant sputtering power, an increase in the atomic mass of the sputtering gas yields larger primary particles on the substrate. However, the aggregate size (as observed by atomic force microscopy) can show the opposite variation because smaller primary particles exhibit greater surface reactivity and greater tendency to aggregate.
(c) Whether the primary particle size increases or decreases with increasing sputtering gas pressure depends on the sputtering voltage and power. At very low pressures, where the mean free path of the sputtered species is comparable to the target-to-substrate separation, a two-dimensionally continuous thin film is formed on the substrate, provided either the substrate temperature is high enough (≈ 300 K) and/or the sputtering voltage is high enough. With increasing gas pressure, the sputtered species are more likely to undergo collision-induced aggregation. At higher pressures, not only do they arrive at the substrate in the form of small atomic/molecular clusters, they also arrive with lower kinetic energies.

A nanocrystalline structure is thereby promoted, particularly if the substrate is unable to provide enough thermal energy for appreciable atomic diffusion.

(d) The sputter-deposited particles may assume a random crystallographic orientation, or a definite orientation dictated by a preferred growth direction. Again, this is dictated by the kinetic energy with which the sputtered species arrive at the substrate and by the thermal energy available there.

In order to obtain structurally reproducible nanomaterials using sputtering, it is necessary to pay attention to certain additional factors. The particle size and orientation are determined not only by the ambient gas pressure but also by the flow rate. The substrate should not be allowed to get heated due to the proximity of the sputtering target, and it may be necessary to protect the substrate periodically by a shutter, using an on-off duty cycle of approximately 30–60 s. It is also necessary to note that the properties of the sputter-deposited samples depend to some extent – rather unfortunately – on the history and surface condition of the target. However, it is relatively simple to use this technique to reduce the average particle size (X-ray domain size) in most materials to about 5 nm through proper choice of substrate temperature, sputtering voltage and gas pressure.

Acknowledgements. It is a pleasure to thank Dr. R Banerjee for several illuminating discussions.

References

1. R.W. Siegel: *In Advanced Topics in Materials Science and Engineering*, ed. by J.L. Moran-Lopez, J.M. Sanchez (Plenum, New York 1993) p. 273
2. C. Suryanarayana: Int. Mater. Rev. **40**, 41 (1995)
3. M.J. Mayo: Int. Mater. Rev. **41**, 85 (1996)
4. K. Lu: Mater. Sci. Eng. **R16**, 161 (1996)
5. A.I. Gusev: Physics Uspekhi **41**, 49 (1998)
6. R.W. Siegel: Ann. Rev. Mater. Sci. **21**, 559 (1991)
7. R.A. Powell, S.M. Rossnagel: PVD for Microelectronics: Sputter Deposition Applied to Semiconductor Manufacturing (Academic, San Diego 1999) p. 2
8. R.K. Singh, J. Narayan: Phys. Rev. B **41**, 8843 (1990)
9. H. Hahn, R.S. Averback: J. Appl. Phys. **67**, 1113 (1990)
10. G.M. Chow, A.S. Edelstein: Nanostructured Materials **1**, 107 (1992)
11. M. Goto, J. Murakami, Y. Tai, K. Yoshimura, K. Igarashi, S. Tanemura: Z. Phys. D **40**, 115 (1997)
12. M. Lal, V. Chhabra, P. Ayyub, A.N. Maitra: J. Mater. Res. **13**, 1249 (1998)
13. A.E. Rakshani: Solid State Electronics **29**, 7 (1986)
14. V.R. Palkar, P. Ayyub, S. Chattopadhyay, M. Multani: Phys. Rev. B **53**, 2167 (1996)
15. R. Chandra, P. Taneja, P. Ayyub: Nanostructured Materials **11**, 505 (1999)
16. P. Ayyub, V.R. Palkar, S. Chattopadhyay, M. Multani: Phys. Rev. B **51**, 6135 (1995)
17. J.A. Thornton: Ann. Rev. Mater. Sci. **7**, 239 (1977)